Available online at www.sciencedirect.com
ScienceDirect
Journal of Environmental Sciences 20(2008) 1028–1034
JOURNAL OF ENVIRONMENTAL SCIENCES
ISSN 1001-0742
CN 11-2629/X
www.jesc.ac.cn

Batch studies of adsorption of copper and lead on activated carbon from *Eucalyptus camaldulensis Dehn.* bark

Phussadee Patnukao[1], Apipreeya Kongsuwan[2], Prasert Pavasant[1,2,*]

1. National Center of Excellence for Environmental and Hazardous Waste Management, Chulalongkorn University, Bangkok 10330, Thailand. E-mail: phussadee@gmail.com
2. Department of Chemical Engineering, Faculty of Engineering, Chulalongkorn University, Bangkok 10330, Thailand

Received 8 September 2007; revised 16 October 2007; accepted 18 March 2008

Abstract

Powdered activated carbon (PAC) prepared from *Eucalyptus camaldulensis Dehn.* bark was tested for its adsorption capacity for Cu(II) and Pb(II). The experiment was conducted to investigate the effects of pH, contact time, initial metal concentration, and temperature. The best adsorption of both Cu(II) and Pb(II) occurred at pH 5, where the adsorption reached equilibrium within 45 min for the whole range of initial heavy metal concentrations (0.1–10 mmol/L). The adsorption kinetics was found to follow the pseudo-second order model where equilibrium adsorption capacities and adsorption rate constants increased with initial heavy metal concentrations. The adsorption isotherm followed Langmuir better than Freundlich models within the temperature range (25–60°C). The maximum adsorption capacities (q_m) occurred at 60°C, where q_m for Cu(II) and Pb(II) were 0.85 and 0.89 mmol/g, respectively. The enthalpies of Cu(II) and Pb(II) adsorption were 43.26 and 58.77 kJ/mol, respectively. The positive enthalpy of adsorption indicated an endothermic nature of the adsorption.

Key words: heavy metal removal; isotherm; kinetics; enthalpy of adsorption; sorption

Introduction

Heavy metal pollutions often are generated from many types of industry, such as electroplating, metal plating, batteries, mining, pigments, stabilizers, alloy industries, and sewage sludge, where the main constituents include copper, lead, nickel, chromium, and so on. Adsorption with activated carbon is one of the most effective techniques for the treatment of such heavy metal containing wastewater. International growing demand of this adsorbent, mainly due to their usages in environmental mitigation applications, has led to a search for new, available low-cost feedstocks with renewable character. Among the potential sources, agricultural wastes stand out as one of the feasible alternatives both in environmental and economical terms. Examples includ the activated carbon derived from rice-hull (Ong *et al*., 2003), coconut shell (Sekar *et al*., 2004), rubber wood sawdust (Kalavathy *et al.*, 2005), apricot stone (Kobya *et al*., 2005), and peanut shell (Wilson *et al*., 2006).

The adsorption capacity obtained from a batch experiment is useful in providing information on the effectiveness of metal-sorbent system. Our previous work demonstrated that the powdered activated carbon (PAC) could well be produced form *Eucalyptus* bark by phosphoric acid activation (Patnukao and Pavasant, 2008). The obtained activated carbon exhibited high surface area (1,239 m^2/g) with high iodine and methylene blue numbers (1,043 and 426 mg/g, respectively). This finding encouraged further investigation focusing on the suitability of this activated carbon for actual treatment systems. Copper and lead ions were therefore selected as modeled pollutants in this study and the dynamic behaviors of the adsorption were investigated to examine the effects of initial metal ion concentration, pH, and the enthalpy of adsorption. Langmuir and Freundlich isotherms were used to fit sorption equilibrium data.

1 Materials and methods

1.1 Preparation of activated carbon

The *Eucalyptus* bark as a raw material was provided by Advance Agro Co., Ltd., Prachinburi Province, Thailand. The raw material was repeatedly washed with tap water, and dried at 105°C for 4 h. The dried bark was impregnated with phosphoric acid (85% by weight) at the weight ratio of 1:1 (bark : acid), and then carbonized in a muffle furnace at 500°C for 1 h. The product was washed with hot distilled water until the pH reached to 6. Finally, the powdered activated carbon was crushed to the size range of 0.045–0.150 mm.

* Corresponding author. E-mail: Prasert.p@chula.ac.th.

1.2 Preparation of metal solutions

Metal solutions were prepared with analytical grade lead nitrate ($Pb(NO_3)_2$), copper nitrate ($Cu(NO_3)_2$), and nitric acid (HNO_3). MilliQTM deionized water was used for all dilution. Metal ion concentrations were measured with AAS (Flame & Graphite Furnace Atomic Adsorption Spectrophotometer, ZEEnit 700, Analytik Jena, UK). The instrument operating conditions (i.e., wavelength and slit width) were set according to the operating manual. Each sample was read four times to get the average value and concentration was corrected for the volume of acid used in sample preparation.

1.3 Batch experiments

Adsorption was performed in batch experiments where 25 ml of heavy metal solutions was added to 0.1 g of activated carbon in conical flasks and mixed with rotary shaker (GFL 3017, Burgwedel, Germany) at 200 r/min. In the adsorption kinetic experiments, the samples were taken to measure the metal concentration at predetermined time intervals (1–60 min). The pH was adjusted in the range from 1 to 6 with adding HNO_3 and NaOH solutions. The sample was then filtered using Whatman No. 42 filter paper and analyzed for the concentration of metal ions remaining in the solution. Initial concentrations of Cu(II) and Pb(II) in the solution were varied from 0.1 to 10 mmol/L. The adsorption isotherm was studied at 25, 40, and 60°C. The metal removal rate (R) is calculated from Eq.(1):

$$R = \frac{(C_i - C_e)}{C_i} \times 100 \quad (1)$$

where, C_i and C_e are initial and equilibrium metal concentrations, respectively. The metal uptake capacity, q, can also be calculated from the difference between the initial and equilibrium concentrations as shown in Eq.(2):

$$q = \frac{(C_i - C_e)V}{M} \quad (2)$$

where, q (mg/g) is the adsorbed metal quantity per gram of activated carbon at any time, M (g) is the adsorbent dosage, and V (L) is the solution volume.

1.4 Sorbent characterization

The activated carbon product was characterized for its functional groups using Fourier Transform Infrared Spectrophotometer (FT-IR) analysis. For this, the activated carbon samples were brought to constant weight in a drying oven at 50°C for 24 h and kept in the desiccators. Then 1 mg dried activated carbon was mixed with 100 mg KBr, which was initially dried at 110°C in the sample disk. The FT-IR spectra were in the range of 450–4000 cm^{-1} (1760X, Perkin Elmer, USA).

2 Results and discussion

2.1 Characterization of activated carbon product

Table 1 summarizes the characteristics of the activated carbon obtained. BET results as shown in Table 1 illustrate that the activated carbon had a relatively high specific surface areas (1,239 m^2/g) with 88.5% micropore and 11.5% mesopore structure. The functional groups, on the surface of activated carbon analysed by FT-IR demonstrated the existence of carboxyl, hydroxyl, and amine groups which were mostly negatively charged. The FT-IR transmission spectra in the range of 450–4000 cm^{-1} for the original activated carbon, the activated carbon laden with Cu(II), and Pb(II) are shown in Fig.1a, 1b, and 1c, respectively. The FT-IR spectroscopic characteristics are shown in Table 2. Fig.1 demonstrates that, after the adsorption, there seemed to be shifts and intensity decreases in wavenumber of dominant peaks. These clear band shifts and intensity decreases could be observed at 3390.59, 1693.14, 1200.85, 1088.49, 828.21, and 500.36 cm^{-1} for Cu(II)-laden activated carbon, and at 3390.59, 1693.14, 1200.85, 517.88, and 500.36 cm^{-1} for Pb(II)-laden activated carbon. These shifts indicated that there were binding processes taking place on the surface of activated carbon (Pavasant *et al*., 2003). The functional groups involved in the adsorption were as follows: broad bands at 3390.59 cm^{-1} representing bonded –OH groups; 2943.07–2866.90 cm^{-1}, the aliphatic C–H group; 2065.57–1693.14 cm^{-1}, the C=O stretching; 1590.93 cm^{-1}, the secondary amine group; 1200.85 cm^{-1}, the C–O stretch; 1088.49 cm^{-1}, the P–O symmetrical vibration in a chain of P–O–P (polyphosphate) which were formed in the carbonized samples in the presence of phosphoric acid, 828.21 cm^{-1} –CN stretching, and 516.88–500.36 cm^{-1} C–C group in alkane. The spectral analysis before and after metal adsorption indicated that –OH groups, C=O stretching, secondary amine group, and symmetric bending of CH_3 were both involved in Cu(II) and Pb(II) adsorption. These functional groups could act as chemical binding agents where carboxyl, hydroxyl, and amine groups could dissociate negatively charged active surface. This meant that these functional groups could attract the positively charge objects such as heavy metal ions (Volesky, 1990). It was worth noting that the functional groups for Cu(II) were also available for the Pb(II) adsorption.

Table 1 Characteristics of activated carbon product from *Eucalyptus* bark

Parameter	Value
Yield (%)	26.2 ± 0.8
Weight loss (%)	54.6 ± 0.5
Apparent (bulk) density (g/cm^3)	0.251
Moisture content (%)	7
Ash content (%)	4.88 ± 0.09
C (%)	76.3
H (%)	1.6
Porous characteristics	
BET specific surface area (m^2/g)	1,239
Micropore (%)	88.5
Mesopore (%)	11.5
Iodine number (mg/g)	1,043 ± 8
Methylene blue number (mg/g)	427 ± 2

2.2 Effect of pH on adsorption

The solution pH affects the adsorbate surface charge and the degree of ionization of the adsorbate speciation,

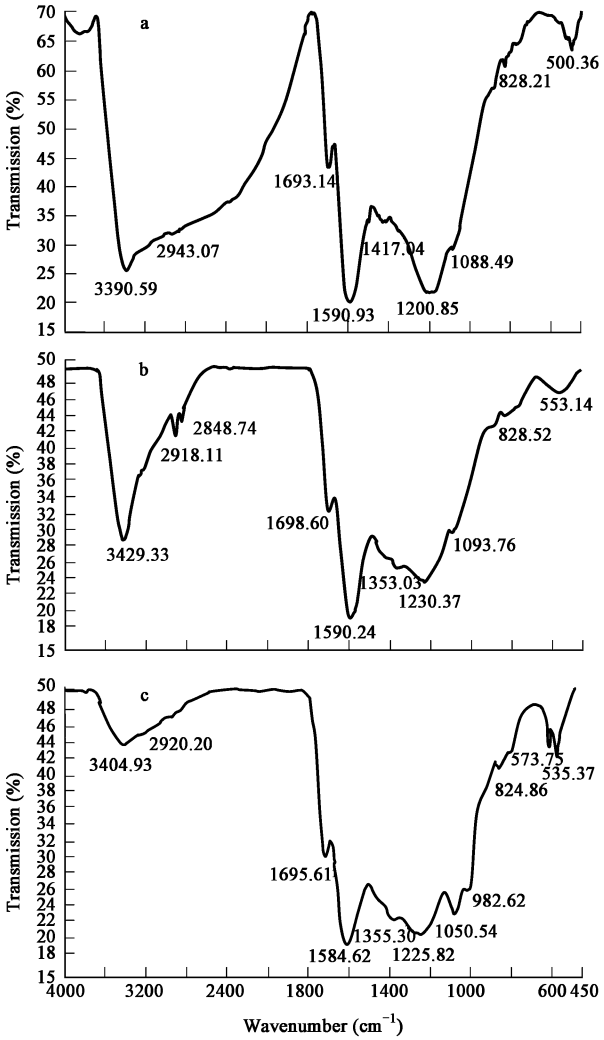

Fig. 1 FT-IR transmission spectra of original activated carbon (a), Cu(II) laden activated carbon (b), and Pb(II) laden activated carbon (c).

therefore, affects the adsorption efficiency of the metal pollutants from wastewaters. Fig.2 demonstrates that the adsorption capacities of Cu and Pb increased with pH. This was attributed to the fact that, at low pH (< 3), the protonation of the active sites at carbon surface was enhanced and this refused the formation of links between

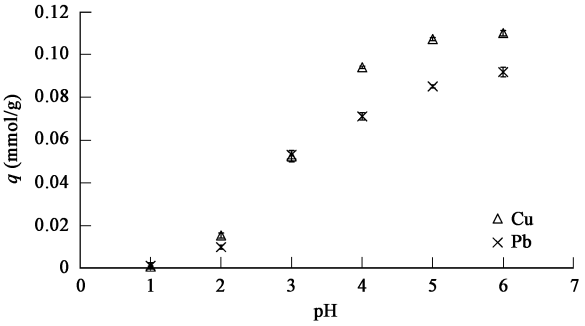

Fig. 2 Effect of pH on adsorption capacity (25°C).

metal ion and the active site. At moderate pH (3–6), linked H^+ was released from the active sites allowing more metal ions to be adsorbed to the vacant sites. Higher pH values (> 6) generally decrease the electrostatic repulsion between cations and also the positively charged surface, which promotes higher adsorption capacity. Therefore, maximum adsorption often occurs at high pH level. However, at this pH range, the formation of insoluble hydrolyzed species $(CuOH)^+$, $(PbOH)^+$, $Cu(OH)_2$, and $Pb(OH)_2$ might also take place, and this condition is often not desirable as the metal precipitation could lead to a misunderstanding for the adsorption capacity.

2.3 Adsorption kinetics

Figure 3 demonstrates the time profiles of the adsorptions of both Cu(II) and Pb(II) onto the activated carbon at different initial concentrations (0.1–10 mmol/L). Generally, the adsorption capacity increased with time until the equilibrium was attained between the amounts of metals adsorbed on the activated carbon and the remaining in the solution. The adsorption took place more rapidly at initial stages and gradually slowed down in reaching its equilibrium state. This behavior is quite common due to the saturation of the available adsorption sites (Yardim *et al*., 2003). The time to reach equilibrium varied with the initial concentration, i.e., the solution with a higher initial concentration required a slightly longer time than the solution with a lower initial concentration. The experiments revealed that the equilibrium was reached

Table 2 FT-IR results from metal laden activated carbon

FT-IR peak	Wavenumber (cm^{-1})					Assignment
	Original adsorption	Cu(II)-loaded activated carbon	Difference[a]	Pb(II)-loaded activated carbon	Difference[b]	
1	3390.59	3429.33	–38.74	3404.93	–14.34	Bonded –OH groups
2	2943.07	2918.11	+24.96	2920.20	+22.87	Aliphatic C–H group
3	2866.90	2848.74	+18.16	2065.57	+801.33	Aliphatic C–H group for 2848.74 cm^{-1} C=O stretching for 2065.57 cm^{-1}
4	1693.14	1698.60	–5.46	1695.61	–2.47	C=O stretching
5	1590.93	1590.24	+0.69	1584.62	+6.31	Secondary amine group
6	1417.04	1353.03	+64.01	1355.30	+61.74	Symmetric bending of CH_3
7	1200.85	1230.37	–29.52	1225.82	–24.97	C–O stretching
8	1088.49	1093.76	–5.27	1050.54	+37.95	P–O
9	828.21	828.52	–0.31	824.86	+3.35	–CN stretching
10	516.88	–	–	573.75	–56.87	Alkane
11	500.36	533.14	–32.78	535.37	–35.01	Alkane

[a] Difference between original adsorption and Cu(II)-loaded activated carbon; [b] differences between original adsorption and Pb(II)-loaded activated carbon.

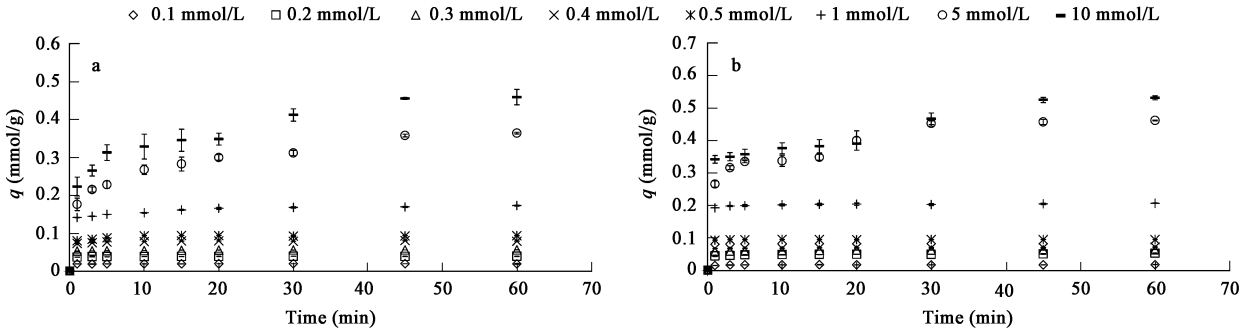

Fig. 3 Adsorption kinetics of Cu(II) (a) and Pb(II) (b) onto activated carbon.

within 45 min for all cases investigated in this work. Fig.3 demonstrates that the kinetic curves were generally smooth and continuous. The saturation could be expected to occur, indicating a monolayer adsorption of metal ion on carbon surface.

To characterize the kinetic behavior, it was common to determine how the rate of reaction varied as the reaction progressed. Lagergren's first order kinetic equation has been most widely used to describe the solute adsorption on various adsorbents, and this can be expressed as Eq.(3) (Lagergren, 1898):

$$\log(q_e - q) = \log q_e - \frac{k_1}{2.303}t \quad (3)$$

where, q_e (mg/g) and q (mg/g) are the amounts of adsorbed metal on the sorbent at the equilibrium and at time t, respectively, and k_1 (min^{-1}) is the rate constant of first-order sorption. Another most widely used kinetic expression is the pseudo-second order rate expression derived by Ho and McKay (2003) where sorption capacity was assumed to be proportional to the number of active sites occupied on the sorbent:

$$\frac{t}{q} = \frac{1}{k_2 q_e^2} + \frac{1}{q_e}t \quad (4)$$

where, k_2 (g/(mg·min)) is the pseudo-second order rate constant.

The experimental data were fitted with these two kinetic models where the kinetic parameters such as rate constants and equilibrium adsorption capacities of adsorption for Cu(II) and Pb(II) are summarized in Table 3. The results illustrated that a linear relationship between $\log(q_e - q)$ and t could not be obtained, indicating that the first order Lagergren rate kinetics might not be appropriate to describe the adsorption. The data seemed to fit much better with the pseudo-second order kinetics where kinetic parameters, q_e and k_2, are summarized in Table 3. Extremely good agreements between the results and the model were obtained as illustrated by the high R^2 for the whole range of initial metal concentrations which, by and large, confirmed the applicability of the pseudo-second order kinetics. Hence, it was concluded at this point that the adsorption here could be better represented by the pseudo-second order rate kinetics.

In addition, the results indicated that an increase in initial metal concentration increased the rate constant (k_2). High k_2 suggested that the metal could be rapidly sequestered by the activated carbon functional groups, resulting in the system quickly reaching equilibrium as reported earlier. This was because an increase in initial metal concentration enhanced the concentration gradient

Table 3 Kinetic parameters of first-order and pseudo-second order models for Cu(II) and Pb(II) adsorption at 25°C

Heavy metal	Initial concentration (mmol/L)	$q_{e,exp}$ (mmol/g)	Pseudo-first order			Pseudo-second order		
			k_1 (min^{-1})	$q_{e,cal}$ (mmol/g)	R^2	k_2 (g/(mmol·min))	$q_{e,cal}$ (mmol/g)	R^2
Cu(II)	0.1	1.97×10^{-2}	4.05	1.92×10^{-2}	0.9976	3.22×10^{-4}	1.94×10^{-2}	0.9997
	0.2	3.91×10^{-2}	3.22	3.86×10^{-2}	0.9995	5.87×10^{-4}	3.90×10^{-2}	1.0000
	0.3	5.63×10^{-2}	3.13	5.51×10^{-2}	0.9971	8.00×10^{-4}	5.64×10^{-2}	1.0000
	0.4	7.99×10^{-2}	2.66	7.84×10^{-2}	0.9962	4.62×10^{-3}	7.95×10^{-2}	0.9998
	0.5	9.11×10^{-2}	2.05	9.16×10^{-2}	0.9882	5.01×10^{-3}	9.36×10^{-2}	0.9999
	1.0	1.73×10^{-1}	2.09	1.61×10^{-1}	0.9695	6.23×10^{-3}	1.74×10^{-1}	0.9997
	2.5	3.00×10^{-1}	1.16	2.72×10^{-1}	0.9368	1.38×10^{-2}	3.10×10^{-1}	0.9998
	5.0	3.66×10^{-1}	0.44	3.10×10^{-1}	0.8604	1.52×10^{-2}	3.77×10^{-1}	0.9930
	10.0	4.59×10^{-1}	0.49	3.86×10^{-1}	0.8468	2.92×10^{-2}	4.79×10^{-1}	0.9900
Pb(II)	0.1	1.74×10^{-2}	2.13	1.72×10^{-2}	0.9966	1.39×10^{-5}	1.77×10^{-2}	0.9995
	0.2	5.30×10^{-2}	2.38	4.94×10^{-2}	0.9892	2.00×10^{-4}	5.23×10^{-2}	0.9988
	0.3	6.45×10^{-2}	2.67	6.18×10^{-2}	0.9937	6.57×10^{-4}	6.42×10^{-2}	0.9993
	0.4	7.10×10^{-2}	3.56	6.92×10^{-2}	0.9978	1.11×10^{-3}	7.10×10^{-2}	0.9996
	0.5	9.40×10^{-2}	3.39	9.19×10^{-2}	0.9386	3.26×10^{-2}	9.56×10^{-2}	0.9997
	1.0	2.00×10^{-1}	3.07	2.02×10^{-1}	0.9967	3.61×10^{-2}	2.07×10^{-1}	0.9997
	2.5	3.89×10^{-1}	0.75	3.55×10^{-1}	0.9330	3.78×10^{-1}	3.97×10^{-1}	0.9997
	5.0	4.25×10^{-1}	0.87	3.96×10^{-1}	0.8562	4.00×10^{-1}	4.80×10^{-1}	0.9998
	10.0	5.30×10^{-1}	1.51	4.24×10^{-1}	0.8079	4.39×10^{-1}	5.51×10^{-1}	0.9996

of metal ion between aqueous and solid phases. Consequently, the mass transfer of adsorbate into adsorbent increased. This finding supported the assumption of the pseudo-second order model that the sorption process was due to chemisorption (Ho, 2003). In this case, chemical sorption could have occurred by the interaction between polar functional groups on the adsorbent surface and the metals.

2.4 Adsorption isotherm

The adsorption isotherms of Cu(II) and Pb(II) ions on activated carbon are illustrated in Fig.4. Adsorption isotherm is the relationship between adsorption capacity and concentration of the remaining adsorbate at constant temperature. Generally, there are two mathematical expressions used to describe the isotherm of the adsorption, Langmuir and Fruendlich equations. Langmuir's isotherm (Langmuir, 1916, 1918) is Eq.(5).

$$\frac{1}{q} = \frac{1}{q_m} + \left(\frac{1}{bq_m}\right)\left(\frac{1}{C_e}\right) \tag{5}$$

where, q_m is the maximum adsorption capacity, b is the Langmuir constant.

Figure 4 illustrates the plots of Cu(II) and Pb(II) ions where a straight line could be well observed between C_e/q_e and $1/C_e$. This indicated that the experimental data followed Langmuir's isotherm. q_m and b were calculated from this plot and the results are summarized in Table 4. The Langmuir parameters, i.e., q_m increased with temperature. High temperatures increased the kinetic energy of the metal and, hence, enhanced the mobility of the metal ions. This led to a higher chance of the metal being adsorbed onto the adsorbent and an increase in its adsorption capacity.

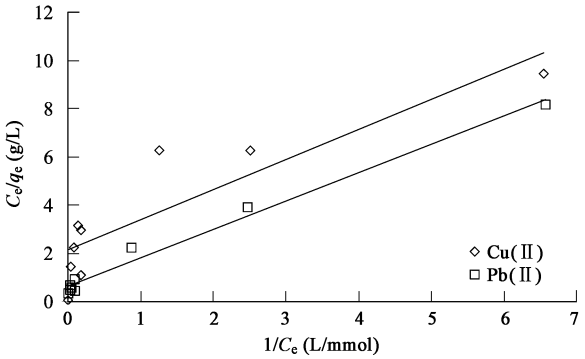

Fig. 4 Langmuir isotherm plots for the adsorption of Cu(II) and Pb(II) onto activated carbon.

The Freundlich isotherm (Freundlich, 1906) is given by:

$$q_e = K_F C_e^{1/n} \tag{6}$$

where, K_F and n are the constants of Freundlich isotherm incorporating adsorption capacity and intensity, while C_e (mmol/g) and q_e (mmol/g) are the remaining concentration of adsorbate after equilibrium and the amount adsorbed at equilibrium, respectively. The Freundlich constants, i.e., $1/n$ and K_F, were calculated from the slope and interception of the Freundlich plots, respectively (Table 4).

As both Langmuir and Freundlich models could explain the adsorption, this suggested that the adsorption of Cu(II) and Pb(II) was potentially monolayer (Feng *et al.*, 2004). The values of $1/n$ of less than 1 confirmed a favorable adsorption onto microporous adsorbent (Faur-Brasquet *et al.*, 2002). The results indicated that activated carbon had higher maximum adsorption capacity for Pb(II). Moreover, Pb(II) adsorption was found to have a higher b value than Cu(II), indicating that this activated carbon had higher affinity for Pb(II) than Cu(II).

2.5 Effect of temperature on metal uptake

The adsorption of Cu(II) and Pb(II) onto activated carbon was favored at higher temperatures as shown in Table 4 and Fig.5. This indicated that chemical adsorption could potentially be the nature of the adsorption of Cu(II) and Pb(II) onto the activated carbon product. The results demonstrated that an increase in the temperature from 25 to 60°C led to an increase in the adsorption capacity from 0.45 to 0.85 mmol/g for Cu(II) and from 0.55 to 0.89 mmol/g for Pb(II), respectively. Adsorption capacities of the activated carbon increased rapidly first with an increase in initial concentrations of Cu(II) and Pb(II) and reached a saturation values of around 10 mmol/L for Cu(II) and Pb(II). Greater removal levels for Cu(II) and Pb(II) were observed at higher temperature range. This was due to the increasing tendency of adsorbate ions to adsorb from the solution to the interface with increasing temperature. The increase of the equilibrium uptake at increased temperature indicated that the adsorption of Cu(II) and Pb(II) ions to activated carbon was endothermic.

2.6 Enthalpy of adsorption

The apparent heat or net enthalpy of adsorption, ΔH, is related to the Langmuir constant, b, as presented in Eq.(7) (Faust and Aly, 1987):

$$\ln b = \ln b' - \frac{\Delta H}{RT} \tag{7}$$

Table 4 Langmuir and Freundlich isotherm parameters for both adsorptions of Cu(II) and Pb(II)

Heavy metal ion	Temperature (°C)	Langmuir isotherm			Freundlich isotherm		
		q_m (mmol/g)	b (L/mmol)	R^2	K_F	$1/n$	R^2
Cu(II)	25	0.45	0.19	0.9911	0.54	0.49	0.9485
	40	0.80	0.58	0.9675	0.07	0.22	0.8373
	60	0.85	1.21	0.9855	0.20	0.44	0.9623
Pb(II)	25	0.55	0.23	0.9969	0.31	0.39	0.7976
	40	0.85	1.87	0.9858	0.38	0.52	0.9413
	60	0.89	2.94	0.9877	0.46	0.46	0.8943

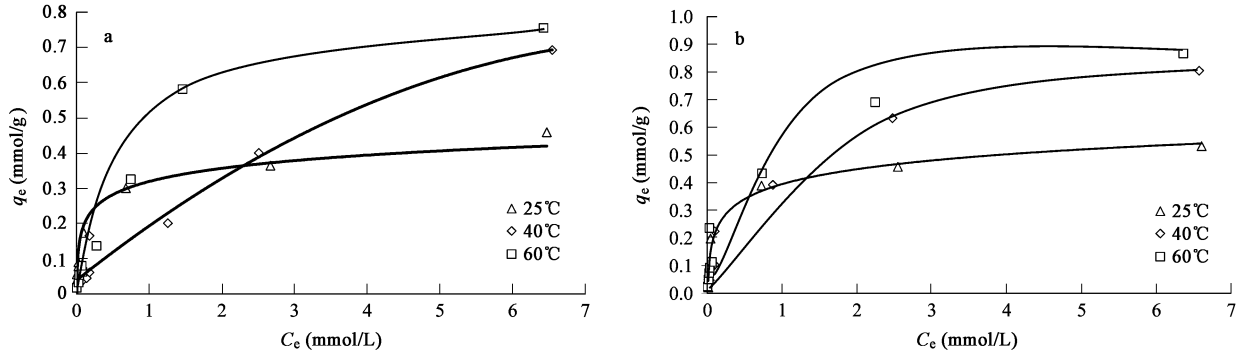

Fig. 5 Adsorption isotherm of Cu(II) (a) and Pb(II) (b) by activated carbon.

where, b' is a constant, R (8.314 J/(mol·K)) is the gas constant, and T is the temperature in Kelvin.

The slopes of the plot of ln$b$ versus $1/T$ of Cu(II) and Pb(II) in Figs.6a and 6b are equal to $-\Delta H/R$ allowing the calculation of H of Cu(II) and Pb(II) to be 43.26 and 58.77 kJ/mol, respectively. The positive enthalpy of adsorption indicated chemical adsorption. This suggested that the chemical bond between the activated carbon surface and the metal ions could not be easily broken by physical mechanism such as simply shaking or heating.

2.7 Comparison of the present study with literature

Table 5 shows various adsorbents previously studied for Cu(II) and Pb(II) removal. It can be seen that the adsorption capacity of the activated carbon from *Eucalyptus* bark was among the highest available which makes the adsorbents suitable for metal removal in actual wastewater facilities. The *Eucalyptus* bark (in this study) could be effectively converted to activated carbon with relatively high levels of BET surface area when compared to other types of raw materials. The difference could be due to the different nature of raw materials (Chen *et al*., 2003), and this led to a different formation of pore structure in the final activated carbon product.

3 Conclusions

The Cu(II) and Pb(II) adsorption by activated carbon from *Eucalyptus* bark was evaluated here. The optimal adsorption of Cu(II) and Pb(II) on the activated carbon occurred at pH 5. The adsorption reached equilibrium within 45 min for the concentration range of 0.1–10 mmol/L and temperature range of 25–60°C. The results on kinetics data was appropriately fitted with the pseudo-second order kinetic model where the adsorption rate constant and equilibrium capacities increased with initial

Table 5 Cu(II) and Pb(II) adsorption capacities of various agricultural-based adsorbents

Adsorbent	Activation method	Surface area (m^2/g)	Adsorption capacity (mmol/g)		Reference
			Cu(II)	Pb(II)	
Cloth-activated carbon	Physical	1,680	0.17	0.15	Faur-Brasquet *et al*., 2002
Activated carbon pretreated with citric acid	Chemical	431	0.23	–	Chen *et al*., 2003
Rice hull-activated carbon	Chemical	–	0.14	–	Ong *et al*., 2003
Coconut-activated carbon	Chemical	266	0.42	–	Sekar *et al*., 2004
Rubber wood sawdust-activated carbon	Chemical	1,674	0.09	–	Kalavathy *et al*., 2005
Apricot stone-activated carbon	Chemical	566	0.38	0.11	Kobya *et al*., 2005
Coconut-granular activated carbon	–	1,000	–	0.11	Goel *et al*., 2005
Coal-activated carbon	–	1,200	–	0.15	Machida *et al*., 2005
Ceiba pentandra hull-activated carbon	Physical	521	0.33	–	Rao *et al*., 2006
Peanut shell-activated carbon	Physical	725	0.84	0.74	Wilson *et al*., 2006
Eucalyptus bark-activated carbon	Chemical	1,239	0.45	0.55	This study

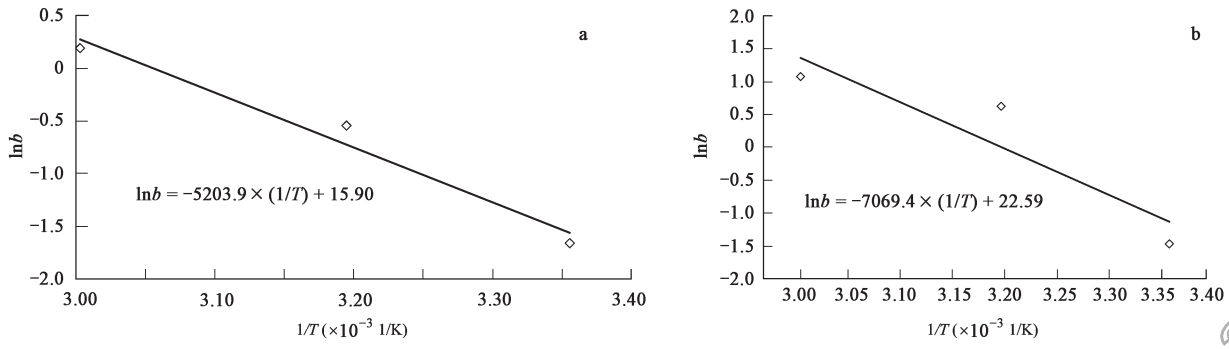

Fig. 6 Plot of ln$b$ versus $1/T$ for Cu(II) (a) and Pb(II) (b)for the determination of adsorption enthalpy.

heavy metal concentration. The adsorption isotherm followed Langmuir better than Freundlich isotherms in the selected range of concentrations, for the whole range of temperature. Activated carbon was found to be an effective adsorbent for the removal of copper (Cu(II)) and lead (Pb(II)) ions where the adsorption capacities of both metals on activated carbon increased with an increase in temperature. The maximum sorption capacities of Cu(II) and Pb(II) adsorption at 60°C were 0.85 and 0.89 mmol/g, respectively, and the positive value of ΔH showed the endothermic nature of adsorption.

Acknowledgments

The authors would like to acknowledge the financial support from the 90th Anniversary of Chulalongkorn University fund (Ratchadphiseksomphot Endowment Fund). The *Eucalyptus* bark was kindly provided by Advance Agro Co., Ltd., Prachinburi Province, Thailand.

References

Chen J P, Wu S, Chong K H, 2003. Surface modification of a granular activated carbon by citric acid for enhancement of copper adsorption. *Carbon*, 41: 1979–1986.

Faur-Brasquet C, Reddad Z, Kadirvelu K, Cloirec P L, 2002. Modeling the adsorption of metal ions (Cu^{2+}, Ni^{2+}, Pb^{2+}) onto ACCs using surface complexation models. *Appl Surf Sci*, 196: 356–365.

Faust S D, Aly O M, 1987. Adsorption Process for Water Treatment. Boston: Butterworths.

Feng Q, Lin Q, Gong F, Sugita S, Shoya M, 2004. Adsorption of lead and mercury by rice husk ash. *J Colloid Interface Sci*, 278: 1–8.

Freundlich H M F, 1906. Over the adsorption in solution. *J Phys Chem*, A57: 385–470.

Goel J, Kadirvelu K, Rajagopal C, Garg V K, 2005. Removal of lead(II) by adsorption using treated granular activated carbon: Batch and column studies. *J Hazard Mater*, B125: 211–220.

Ho Y S, 2003. Citation review of Lagergren kinetic rate equation on adsorption reactions. *Scientometrics*, 59(1): 171–177.

Ho Y S, McKay G, 2003. Pseudo-second order model for sorption processes. *Process Biochem*, 34(5): 451–465.

Kalavathy M, Karthikeyan T, Rajgopal S, 'Miranda L R, 2005. Kinetic and isotherm studies of Cu(II) adsorption onto H_3PO_4-activated rubber wood sawdust. *J Colloid Interface Sci*, 292: 354–362.

Kobya M, Demirbas E, Senturk E, Ince M, 2005. Adsorption of heavy metal ions from aqueous solutions by activated carbon prepared from apricot stone. *Biores Technol*, 96: 1518–1521.

Lagergren S, 1898. About the theory of so-called adsorption of soluble substances. *Kungliga Svenska Vetenskapsakademiens*, *Handlingar*, 24: 1–39.

Langmuir I, 1916. The constitution and fundamental properties of solids and liquids. *J Am Chem Soc*, 38(11): 2221–2295.

Langmuir I, 1918. The adsorption of gases on plane surfaces of glass, mica and platinum. *J Am Chem Soc*, 40(9): 1361–1403.

Machida M, Aikawa M, Tatsumoto H, 2005. Prediction of simultaneous adsorption of Cu(II) and Pb(II) onto activated carbon by conventional Langmuir type equations. *J Hazard Mater*, B120: 271–275.

Ong S A, Lim P E, Seng C E, 2003. Effects of adsorbents and copper(II) on activated sludge microorganisms and sequencing batch reactor treatment process. *J Hazard Mater*, B103: 263–277.

Patnukao P, Pavasant P, 2008. Activated carbon from *Eucalyptus camaldulensis Dehn* bark using phosphoric acid activation. *Biores Technol*, 99(17): 8540–8543.

Pavasant P, Apiratikul R, Sungkhum V, Suthiparinyanont P, Wattanachira S, Marhaba T, 2003. Biosorption of Cu^{2+}, Cd^{2+}, Pb^{2+} and Zn^{2+} using dried marine green macroalga *Caulerpa lentillifera*. *Biores Technol*, 97: 2321–2329.

Rao M M, Ramesh A, Rao G P C, Seshaiah K, 2006. Removal of copper and cadmium from the aqueous solutions by activated carbon derived from *Ceiba pentandra* hulls. *J Hazard Mater*, B129: 123–129.

Sekar M, Sakthi V, Rengaraj S, 2004. Kinetics and equilibrium adsorption study of lead(II) onto activated carbon prepared from coconut shell. *J Colloid Interface Sci*, 279: 307–313.

Volesky B, 1990. Biosorption of heavy metal. Boston: CRC Press.

Wilson K, Yang H, Seo C W, Marshall W E, 2006. Select metal adsorption by activated carbon made from peanut shells. *Biores Technol*, 97: 2266–2270.

Yardim M F, Budinova T, Ekinci E, Petrov N, Razvigorova M, Minkova V, 2003. Removal of mercury(II) from aqueous solution by activated carbon obtain from furfural. *Chemosphere*, 53: 835–841.